

AnnexinA2 and A6 interact with the first exon of tau contributing to tau's axonal localization

Anne Gauthier-Kemper^{a*}, María Suárez Alonso^{c,d*}, Frederik Sündermann^a, Benedikt Niewidok^a, Maria-Pilar Fernandez^c, Lidia Bakota^a, Jürgen Josef Heinisch^b, Roland Brandt^{a#} (*both authors contributed equally)

^aDepartment of Neurobiology, and ^bDepartment of Genetics, University of Osnabrück, D-49076 Osnabrück, Germany, ^cDepartment of Biochemistry and Molecular Biology, Faculty of Medicine, University of Oviedo, 33006 Oviedo, Spain, ^dCurrent address: Department of Physiology/Medicine, University of Fribourg, Chemin du Musée, 5, 1700 Fribourg, Switzerland

Running title: *Annexin-tau interaction*

[#]To whom correspondence should be addressed: Prof. Dr. Roland Brandt, Department of Neurobiology, University of Osnabrück, Barbarastraße 11, D-49076 Osnabrück, Germany, phone: [+49](541)969-2338, FAX: [+49](541)969-2354, e-mail: brandt@biologie.uni-osnabrueck.de

Keywords: tau protein, microtubule-associated protein, annexin, polarity, axon

ABSTRACT

During neuronal development, the microtubule-associated protein tau becomes enriched in the axon where it remains concentrated in the healthy brain. In tauopathies such as Alzheimer's disease, tau redistributes from the axon to the somatodendritic compartment. However, the cellular means of regulating tau's localization remains unclear. We report that tau interacts with the Ca²⁺-regulated plasma membrane-binding protein annexin A2 (AnxA2) via the first coding exon (E1) of its amino-terminal projection domain. Bioinformatic analysis identifies two conserved 8-amino-acid-long motifs within E1 in mammals. Disease-related mutations and pseudophosphorylation of tyrosine 18, which are located within E1 but outside of the conserved regions, do not influence tau's interaction with AnxA2. Tau interacts with the core domain of AnxA2 in Ca²⁺-induced open conformation and interacts also with AnxA6. Presence of E1 moderately reduces the availability of tau to interact with microtubules. Competition by overexpression of constructs containing E1 compromise tau's axonal enrichment in primary neurons. Our data suggest a role of the tau-annexin interaction through E1 in contributing to the enrichment of tau in the axon and its redistribution during pathology.

The tau proteins belong to the tau/MAP2/MAP4 family of microtubule-associated proteins (MAPs), which share a similar microtubule-binding region at their C-terminal end (1). Tau and MAP2 are predominantly present in neurons, whereas MAP4 is a non-neuronal MAP. While MAP2 is mainly localized in the somatodendritic compartment, tau becomes enriched in axons early during the development of polarity and remains concentrated in this compartment in the healthy brain (2-4). The compartment-specific distribution of the neuronal MAPs may have a role in regulating the balance of microtubule-dependent transport in axons versus dendrites (5). Remarkably, during development of tauopathies such as Alzheimer's disease (AD), tau redistributes from the axon to the somatodendritic compartment where it aggregates into filamentous structures (paired or straight helical filaments), which form neurofibrillary tangles (NFTs) (6). The enrichment of tau in the axon may at least partially be mediated by the axon initial segment (AIS), which is thought to act as a selective diffusion barrier for various proteins (7-9) In fact, the integrity of the AIS is disrupted in animal models of AD (10), which may contribute to the pathologic mislocalization of tau during disease. However, it is still a matter

of debate how tau becomes enriched in the axon, how it is retained in this compartment, and what causes its redistribution during disease.

Tau belongs to the class of intrinsically disordered proteins (IDPs), which are known to interact with a large number of unrelated partners. As such, a minimal interactome of 73 binding partners have been estimated (11). In tau immunoprecipitates, >500 proteins have been identified by mass spectrometry (12) however it is unclear to what extent this number reflects proteins, which directly interact with tau. It is likely that interactions other than tau's binding to microtubules are involved in retaining tau in the axonal compartment since microtubules are ubiquitously present in neurons and tau shows a highly dynamic interaction with microtubules (13,14). Such a dynamic interaction would result in a rapid redistribution of tau in the cell, if microtubules would be the sole interaction partner of tau. Therefore, the identity of tau's interaction partner(s) in the axon and how they might contribute to tau's localization still needs to be revealed.

It is known since some time that tau interacts with components of the neuronal plasma membrane through its non-microtubule binding projection domain (15). Such an interaction could provide a specific mechanism to retain MAP tau rather than other MAPs in the axonal compartment, the latter being characterized by a high (membrane) surface to volume ratio close to a high density microtubule array. We have previously shown that the tip of a neurite acts as an adsorber trapping tau protein and that binding was mediated by tau's aminoterminal projection domain (16). We also identified the membrane-binding protein annexin A2 (AnxA2) as a potential interaction partner of tau (17). However it is not known how tau interacts with AnxA2 and which regions of the two proteins are involved in binding.

The annexins constitute a multigene family of Ca^{2+} -regulated membrane binding proteins, which are thought to organize the interface between the cytoplasm and the cytoplasmic face of cellular membranes (18). In vertebrates, 12 annexin subfamilies (A1-A11 and A13) have been identified. The Ca^{2+} -dependent membrane interaction occurs through the annexin core domain as a conserved binding

module. The N-terminal region precedes the core domain and is diverse in length and sequence between the different members of the annexin family (19). AnxA2 and A6 have been shown to reside in lipid rafts and, in particular, AnxA2 appears to be involved in organizing cholesterol-rich microdomains and linking them to cytoskeletal proteins (20). In neurons, AnxA2 is present in high concentrations in growth cones and axonal branches (21). AnxA6 becomes concentrated in the AIS during neuronal development (22). Its presence in the AIS is independent of neuronal activity and resistant against detergent extraction consistent with an interaction with cytoskeletal proteins (23). Interestingly, in pathological states the expression of AnxA6 is altered and its distribution is changed (24,25). If tau only interacts with AnxA2 or also with AnxA6 is not known.

In this study we mapped the interaction of tau with AnxA2 and AnxA6 using a heterologous yeast system. We identified the extreme N-terminus of tau as interaction site and demonstrated that the interaction is not affected by familial tau mutations in the first coding exon (E1) or by introducing a phospho mimicking or blocking mutation of tyrosine 18. By bioinformatic analysis we identified two motifs that are conserved in mammals but are absent in fish. Using an in-cell competition assay, we provide evidence that the interaction via E1 is involved in tau's axonal retention. We believe that our results contribute to an understanding of the processes, which lead to the enrichment of tau in the axon and are involved in its redistribution during pathology.

RESULTS

Tau's amino-terminal projection domain interacts with annexin A2.

Previously, we have identified the calcium-regulated plasma membrane-binding protein annexin A2 (AnxA2) as an interaction partner of tau by tandem-affinity purification tag purification and mass spectroscopy (17). Notably, the interaction required the presence of Ca^{2+} . To systematically identify the interacting domain and potential regulatory mechanisms involved in the binding, we employed pull-down assays in a heterologous yeast expression

system. The choice to use a yeast system was motivated by our previous observations using mammalian cell lines that the presence of Ca^{2+} resulted in unspecific precipitation of AnxA2 in neural cell lysates under control conditions, probably due to the formation of unspecific complexes in the presence of neural membrane components (17).

We first confirmed the interaction of full-length tau ($\text{Flag}\tau_{441\text{wt}}$) with GFP-tagged human AnxA2 in the heterologous yeast system (Fig. 1A, left). In a control experiment where tau was co-expressed with GFP alone, tau did not precipitate (Fig. 1A, right). To test whether we could reproduce the calcium-dependency of the interaction also in the heterologous yeast expression system, we performed the same pull-down experiment in the absence of Ca^{2+} . Indeed, tau did not co-precipitate with AnxA2 under these conditions (Fig. 1A, bottom).

For detection of tau we used an antibody (Tau5), which recognizes an epitope in the middle of the protein (aa 218-225; (26)) since the Flag-tag allowed only inefficient detection in immunoblots. To be able to detect also constructs that did not contain the Tau5-epitope, we prepared a panel of tau deletion constructs with an amino-terminal tandem human influenza hemagglutinin (HA)-tag for immunodetection with an anti-HA antibody. We confirmed that the presence of the short tag (18 aa) did not interfere with tau's binding to AnxA2 (Fig. 1B top). 2HA-tagged tau constructs were therefore employed in further experiments. To map the interaction to a specific region within tau, we first split tau into two parts. A tau fragment containing the N-terminal projection region and the proline-rich region (PRR; aa 1-255) showed interaction, while the carboxy-terminal half containing the microtubule-binding region (MBR) and the carboxy-terminal region (CTR) did not. A further truncation of the aminoterminal half showed that the N-terminal projection region (1-171) was sufficient to bind to AnxA2. To test whether the first expressed exon (E1) was sufficient for the tau-AnxA2 interaction, we prepared a construct with a carboxyterminal fusion to the cytosolic yeast protein Gpm1 (phosphoglycerate mutase) as a carrier, since the remaining tau alone was not stably produced in yeast. We observed that the

fusion construct containing E1 co-precipitated with AnxA2, while the HA-tagged carrier alone (2HA-Gpm1) did not. To exclude a potential influence of the Flag-epitope on binding we prepared an additional construct lacking the Flag sequence (2HA-tau(1-44)-Gpm1). Also this construct co-precipitated with AnxA2, indicating that the sequence which is encoded by tau's first exon is sufficient for tau's binding to AnxA2. This is also consistent with our previous observation that fetal as well as adult tau bind to AnxA2, because E1 (in contrast to the alternatively spliced exons 2 and 3 at the aminoterminal) is present in all isoforms. Constructs containing the PRR but lacking the projection domain could not be tested since they tended to nonspecifically precipitate in our pull-down assays probably due to high aggregation propensity (data not shown).

Tau's first coding exon contains evolutionarily conserved sequence motifs.

Although tau, at least in its non-phosphorylated state, is a basic protein, E1 is acidic with a theoretical pI of 4.26. To determine whether tau's first coding exon contains sequence motifs, which are evolutionarily conserved and may therefore also be of functional relevance, we performed bioinformatic analyses. We performed subHMM analysis of the pHMM from 49 mammalian full length sequences of MAPT (27). We identified two 8aa-long motifs, which are highlighted in Fig. 2A, top. By comparing these motifs with the pHMMs of birds, reptiles and ray-finned fishes (Actinopterygii) we could follow their development during evolution. None of the two motifs were present in ray-finned fishes, while motif I was clearly evident also in reptiles, and, with a much lower expectation value, in birds (Fig. 1A, right). The fact that motif II is exclusively present in mammalian sequences may indicate that it represents a functional region peculiar to mammalian evolution. Motif I showed a clear overrepresentation of negatively charged amino acids (glutamate, aspartate) suggesting an involvement in protein-protein interactions through electrostatic forces.

Tau's binding to annexin A2 is not affected by disease-associated mutations and phospho

mimicking or blocking mutations of tyrosine 18 within E1.

The interaction between tau and annexin might be influenced by disease-associated mutations or phosphorylation in some amino acid residues from the first coding exon. Previously mutations of arginine at position 5 (R5H, R5L) had been observed in tauopathies (28,29) and phosphorylation of tyrosine 18 had been reported in paired helical filaments from AD brains (30). To test an effect of these modifications on the tau-annexin interaction, we performed pull-down assays from yeast extracts containing tau's N-terminal projection region with R5H and R5L-mutations as well as phosphorylation-mimicking and -blocking mutations at tyrosine 18 (Y18E, Y18F). We observed that all constructs co-precipitated with AnxA2 to a similar extent indicating that the mutations do not affect the interaction of tau with AnxA2 (Fig. 2B). Noteworthy, both residues are located outside of the evolutionarily conserved motifs in E1 and the data suggest that the tau-annexin interaction is robust against changes in these positions. So far, no changes, which would be located within the two conserved regions, have been described.

Tau binds to the core domain of AnxA2 in its Ca²⁺-induced open conformation and interacts also with annexin A6.

Annexins consist of a conserved Ca²⁺- and membrane-binding core domain and a preceding N-terminal region, which is diverse in sequence and length ((19); Fig. 3A, left). To test which part of AnxA2 interacts with tau, we prepared deletion constructs coding only for the N-terminal region (aa 1-34) or the core domain (aa 35-339) of AnxA2, both as C-terminal GFP fusions for co-precipitation assays. We observed that tau co-precipitated with the construct coding for the core domain but failed to do so with the N-terminus of AnxA2 (Fig. 3A, right). AnxA2 is known to exist in a closed (absence of Ca²⁺) and an open conformation (presence of Ca²⁺) and the N-terminal region may mask tau's binding site to the AnxA2 core domain in the closed conformation (31). Therefore, to test whether the interaction between tau and annexin's core domain remained Ca²⁺-dependent also in the absence of the N-terminal region, we performed

co-precipitation assays of tau's N-terminal projection region with the construct coding for annexin's core domain in the presence and absence of Ca²⁺. In fact, we observed that binding to the AnxA2 core domain is independent of the presence of Ca²⁺ (Fig. 3B).

The core domain, which consists of the annexin repeats, is conserved among the different annexin subfamilies. Since we have shown that tau binds to the core domain of AnxA2 it might also interact with other members of the annexin family. In mammalian neurons, AnxA6 might be an interesting candidate due to its presence in the axon initial segment (AIS). Indeed, tau's N-terminal projection region clearly co-precipitated with AnxA6 after expression in the heterologous yeast system indicating physical interaction (Fig. 3C). To confirm that the interaction occurs via E1 and to test for a potential Ca²⁺ dependency, we performed pull down assays also with the 2HA-tau(1-44)-Gpm1 construct with AnxA6 in the presence and absence of Ca²⁺. We observed that the construct co-precipitated with AnxA6 in the presence of Ca²⁺, while it failed to do so without Ca²⁺ (Fig. 3D).

Lack of E1 moderately increases tau's association rate in axon-like processes.

As demonstrated, the E1 region of tau is involved in binding of tau to the plasma membrane components AnxA2 and AnxA6. In order to test whether this additional interaction affects tau's interaction with microtubules, we prepared a tau construct lacking E1 (tau_{ΔE1}) and compared it with the behavior of full-length tau (tau_{wt}), both as PAGFP-tagged versions. The constructs were present as single polypeptides in transfected PC12 cells, indicating their integrity (Fig. 4A, left). The difference in electrophoretic mobility was much higher than calculated from the sequence (16.9 versus 5.2 kDa) suggesting that E1 largely contributes to the unusual low electrophoretic mobility of tau protein and forms a stiff domain. To scrutinize the interaction of the two constructs with microtubules in axon-like processes of living cells, we used a fluorescence decay after photoactivation (FDAP) approach (Fig. 4A, right). We had previously shown that the PAGFP-fusion does not interfere with tau's interaction with axonal

membrane components (16,17). After neuronal differentiation of transfected PC12 cells, PAGFP was activated within a segment in the middle of the process by a laser flash at 407-nm wavelength and FDAP was recorded in the activated region as a function of time. Both constructs showed a much slower decay than a non MT-binding control protein of similar size (3×PAGFP) indicating binding to microtubules (Fig. 4B). Based on the effective diffusion constants, >90% of the constructs were bound to microtubules, which is consistent with previous data on the tau-MT interaction in processes of living cells (16,32). To directly estimate the pseudo-first-order association rate ($k_{on}^* = k_{on}[MT]_{eq}$, where $[MT]_{eq}$ is the equilibrium concentration of tau-binding sites on MTs) and the dissociation rate (k_{off}), we used a previously developed refined reaction-diffusion model of the tau-MT interaction (33). Absence of E1 led to a moderate but significant increase in k_{on}^* but did not influence k_{off} (Fig. 4C), which is consistent with the slight decrease in FDAP of $\tau_{\Delta E1}$ compared to τ_{wt} (Fig. 4B). The data are consistent with the supposition that the presence of the tau-annexin interaction moderately reduces the availability of tau to interact with MTs (as indicated by the lower k_{on}^* value of τ_{wt} compared to $\tau_{\Delta E1}$) but does not affect its dwell time (the inverse value of k_{off}), once tau is bound on the MT surface.

Competition with the tau-annexin interaction compromises tau's axonal enrichment.

AnxA2 is present in high concentrations in neuronal growth cones while AnxA6 becomes concentrated during development in the axon initial segment (AIS) (21,22). This localization could implicate a contribution of the tau-annexin interaction to tau's retention in the axon. To test this hypothesis we prepared Sindbis Virus (SV) constructs providing transient overexpression of the interacting domain in order to compete with a potential interaction of endogenous tau with annexin in living primary cortical neurons. We prepared a fusion construct of tau's E1 with triple mCherry (3×mCherry) as a fluorescence marker, and a second construct, where we added E2 as a spacer between E1 and the fluorescence marker. As a control, we used 3×mCherry alone. Based on Western Blot analysis, we estimated a

level of overexpression of the constructs compared to endogenous tau protein of at least 3-fold.

Similar to its distribution in the brain, endogenous tau shows enrichment in one process in cultured primary neurons, which could be identified as axon by morphological criteria (3). SV-mediated expression of the control construct (3×mCherry) did not change this distribution and the majority of infected neurons showed endogenous tau-staining, which was largely restricted to the axon (Fig. 5A, top, arrowhead). In contrast, after expression of the competing constructs coding for E1, or E1 and E2, most of the infected neurons lost the preferential staining of endogenous tau in the axon and the tau signal was present in multiple processes (Fig. 5A, middle and bottom). Quantification confirmed that overexpression of the competing constructs abolishes the preferential distribution of endogenous tau in one process (Fig. 5A, right; $F(2,9)=179.3$, $p<0.001$) suggesting that tau's interaction via its first coding exon contributes to its enrichment in the axon.

To determine whether the overexpression of constructs containing E1 influence axonal integrity in general, we performed similar infection experiments and stained for the distribution of the somatodendritic marker MAP2, which is known to segregate into dendrites after development of polarity (34) (Fig. 5B). We observed axonal exclusion of MAP2 in the vast majority of neurons after expression of the control construct (3×mCherry), which did not change with constructs containing E1, suggesting that overexpression of E1 specifically affected the distribution of tau.

DISCUSSION

We have previously shown that the neuronal microtubule-associated protein tau interacts with the calcium-regulated plasma membrane-binding protein annexin A2 (AnxA2) however the interaction sites of both proteins and potential functional consequences remained unknown. In this study, we mapped the tau-annexin interaction using a heterologous yeast system, performed bioinformatic analysis of the interacting tau domain and applied an in-cell

competition assay to determine effects on the localization of tau. Our major findings are as follows: (1) tau interacts with AnxA2 via E1 of its amino-terminal projection domain, (2) tau binds to the core domain of AnxA2 in the Ca^{2+} -induced open conformation and interacts also with AnxA6 via E1, and (3) competition with the tau-annexin interaction compromises tau's axonal enrichment.

Tau belongs to the class of IDPs, which are known to interact with many partners (11). While the carboxy-terminal half containing the microtubule-binding region (MBR) is very similar among the members of the tau/MAP2/MAP4 family (27,32), interactions of tau's amino-terminal projection domain, which extends from the MT surface when tau is bound to microtubules, are likely to mediate the more specific interactions of tau. We have previously shown that tau's projection domain mediates enrichment of tau at distal neurites, probably via interaction with plasma membrane components (15,16,35). A recent proteomic study indicated that various membrane-bound proteins interact with N-terminal inserts of tau, providing further evidence for potentially relevant interactions of tau's projection domain with membrane components (36). In this study, we have identified tau's first coding exon as the region, which interacts with AnxA2 in a Ca^{2+} -dependent manner. E1 exhibits the maximum distance from tau's MBR with a spacing of ~19 nm from the microtubule surface, from which the projection domains extend as arm-like elements according to previous electron microscopic studies (37) (Fig. 6A). Thus, E1 is well positioned to bridge microtubules with plasma membrane components, which may be of particular importance for the axonal compartment, where the membrane surface to volume ratio is highest. Alternatively or in addition, AnxA2-bound tau could represent an additional pool of axonal tau thereby reducing the amount of tau, which is available for the interaction with microtubules that is known to be highly dynamic in axons (14). This is consistent with our observation that a truncated construct of tau, which lacks E1 and is therefore incapable of interacting with AnxA2, shows a moderately increased k_{on}^* rate of microtubule binding compared to wildtype tau (see Fig. 4C). It should however be noted

that also other factors may affect the change in tau's microtubule interaction, e.g., binding of E1 to components other than annexins or induction of structural changes of tau.

Tau is subject to a variety of post-translational modifications and can carry disease-associated mutations, some of which are located in E1 (38). Phosphorylation of tyrosine 18, which is located between two 8aa-long conserved motifs, which we identified by bioinformatic analysis, had been observed in paired helical filaments from AD brains (30) and phosphorylation of this residue may be involved in regulating axonal transport (39). Mutations of arginine at position 5 had been identified in a late age of onset case of FTDP-17 (R5H; (28)) and progressive supranuclear palsy (R5L; (29)). We observed that both phospho blocking and mimicking tau mutants at Tyr-18 bound to AnxA2 indicating that the interaction is robust against a negative charge at this position. We also did not observe a change in the annexin interaction of the disease-associated mutations R5H and R5L. It would be informative to model the interaction between tau's E1 and AnxA2 in order to identify other critical residues and to deduce, which modifications may affect the tau-annexin interaction. However, our attempts to predict the 3D structure of tau's E1 using popular (and one of the most efficient) tools like QuickPhyre and Tasser were unsuccessful. Both algorithms reported that the fraction of potential unordered regions is highly flexible and thus did not allow the construction of a suitable 3D model. For the time being, this impedes the presentation of an adequate tau-annexin interaction model.

We observed that the interaction of tau with AnxA2 depended on the presence of Ca^{2+} . It had previously been suggested that annexin exists in a closed (no Ca^{2+} , no membrane) and an open conformation (in the presence of Ca^{2+} and membrane binding). In the closed conformation, the N-terminal region is thought to integrate into the folded core, while Ca^{2+} - and membrane binding can then trigger exposure of the N-terminal region in the open conformation (31). This implies that Ca^{2+} may be required for making annexin's core domain available for the interaction with tau (Fig. 6A). In support of such a hypothesis, we observed that tau interacts with

the core domain of AnxA2 and that the tau-AnxA2 interaction becomes Ca^{2+} -independent, when the N-terminal region is removed. Interaction with the annexin core domain as a conserved binding module also implied that tau may bind to other members of the annexin family. In mammalian neurons, especially AnxA6 might be an interesting candidate because it is present in the axon initial segment (AIS) and shows an altered distribution in pathological states (23,25). Indeed, we here observed that tau also binds to AnxA6 via E1 of its amino-terminal projection domain in a Ca^{2+} -dependent manner in the heterologous yeast system. Notably, AnxA6 is the only annexin that contains two annexin core domains within a single physical entity (18), which may imply that even two tau proteins bind to one molecule of AnxA6 (Fig. 6B).

Members of the tau/MAP2/MAP4 family share the conserved carboxy-terminal domain containing the microtubule-binding region (MBR) (27), but exhibit distinct localizations in cells pointing to a role of the aminoterminal in mediating proper subcellular localization. This is evident for the neuronal MAPs tau and MAP2, which exhibit an axonal and somatodendritic distribution, respectively. Our data provide evidence that the interaction of tau's aminoterminal projection domain with neuronal annexins through E1 contributes to its axonal localization. We have shown that E1 contains two 8aa-long sequence motifs (motif I and II; Fig. 2A), which are evolutionary conserved and may therefore also be of functional relevance. Notably, both motifs were absent in fish tau, which may indicate that certain interactions of tau developed later during evolution, when nervous systems became more complex and tau and MAP2 developed compartment-specific functions. This may explain the observation that, unlike the predominantly axonal localization of tau in most mammalian species *in situ*, exogenously expressed tau was equally found in all compartments of lamprey anterior bulbar cells (ABCs), the most studied neurons in sea lampreys (40). Supporting this view, no evidence for axon-specific localization of tau has been reported in zebrafish (41). Interestingly, among mammals, naked mole-rats

(NMRs) maintain axonal tau localization during their extraordinary long life time (~32 years) indicating effective mechanisms of axonal retention (42). Motif I is highly conserved in tau from NMRs, while motif II is partially absent suggesting that motif I has a primary role in keeping tau in the axon.

It is thought that the AIS play a role in the selective localization of tau in the axonal compartment (7,9). We hypothesize that the interaction of tau with annexins, in particular with AnxA6 which is enriched in the AIS, generates a bottle neck, which leads to retention of tau in the axonal compartment of higher vertebrates (Fig. 6B). It was previously reported that axonal retention requires binding of tau to microtubules and that tau redistributes when it is phosphorylated in its repeat domain and detached from microtubules (Li et al., 2011). This indicates a requirement for both, interaction with annexins *and* microtubule binding, for tau's axonal retention.

Gene-edited endogenous tau also displays strong axonal enrichment, which is distorted when exogenous tau is overexpressed (43), consistent with a competition for annexin or MT binding. Remarkably, recent data also indicate that transgenic expression of tau causes a relocation of the AIS down the axon (44). This suggests that the AIS does not only influence tau distribution but that tau also influences the structure of the AIS. Whether such an effect is mediated via tau's interaction with annexins or whether other interaction partners are involved needs to be shown.

Our results may also contribute to an understanding of the processes, which are involved in tau's redistribution during pathology, where tau leaves the axon and becomes enriched in the somatodendritic compartment. Aging alone does not appear to affect the structure of the AIS and the localization of tau, at least not in an aged rat model (45). However during disease conditions, tau is subject to proteolytic cleavage by the Ca^{2+} -activated cysteine protease, calpain, which is activated by $\text{A}\beta$ and cleaves tau at lysine 44 (K44) and arginine 230 (R230) producing tau fragments with potential neurotoxicity (46-48). Calpain-mediated cleavage at K44 would produce a tau fragment lacking E1, which would

be defective in interacting with annexins thereby losing axonal retention. In addition, disease-associated posttranslational modifications may disturb the tau-annexin interaction. A potential candidate is tau acetylation, which has been shown to cause a miss-sorting of tau into the somatodendritic compartment associated with a perturbation of the AIS (9). Finally, a disturbed calcium homeostasis, which is known to be associated with several neurodegenerative diseases (49), may be a common mechanism underlying pathological changes since we have shown that calcium is required for the binding of tau to the neuronal membrane via annexins.

EXPERIMENTAL PROCEDURES

Materials and antibodies

Chemicals were obtained from Sigma-Aldrich, cell culture media and supplements from Sigma-Aldrich and Invitrogen, and culture flasks, plates, and dishes from Thermo Fisher Scientific, unless stated otherwise. Synthetic yeast media were from Becton, Dickinson and Co. (Sparks, USA) and applied as described previously (50). The following antibodies were used: anti-tau (Tau-5 (mouse; BD); ab75714 (chicken; Abcam, UK)), anti-GFP (rabbit; Invitrogen), anti-AnnexinA2 (H-5; mouse; Santa Cruz Biotechnology, Inc.); anti-HA (rat and mouse; kindly provided by Anja Lorberg, University of Osnabrück). As secondary antibodies, peroxidase-conjugated goat anti-mouse and goat anti-rabbit (Jackson ImmunoResearch Laboratories, Inc.), and Alexa Fluor 488-conjugated goat anti-chicken antibodies (ab150173, Abcam, UK) were used.

Construction of expression vectors and Sindbis virus preparation

Eukaryotic expression plasmids for tau441wt (τ_{wt}) with amino-terminally fused PAGFP-tag were constructed in pRc/cytomegalovirus (CMV)-based expression vectors (Life Technologies, Carlsbad, CA) containing a CMV promoter and kanamycin and neomycin resistance genes. Deletion of E1 from tau (τ_{wt}) generating $\tau_{\Delta E1}$ was achieved by using site-directed mutagenesis with the following primers: forward 5'-TCTCCCCTGCAGACCCCC-3' and reverse 5'-AGATCTGAGTCCGGACTTGTACAG-3'. The pCMV-3×PAGFP plasmid was described

previously (16). Sequences for 3×mCherry (pJH1295, with the fluorophore obtained by PCR from pCM79 (51)), Tau(1-44) (pJH1601) and Tau(1-75) (pJH1602) were cloned into pSinRep5 vector. The pSinRep5 vectors and helper DH(26S)DNA were then transcribed *in vitro*, co-electroporated into baby hamster kidney (BHK-21) cells, and pseudovirions were harvested as described previously (52).

Cell culture, transfection and infection

PC12 cells were cultured in serum-DMEM and transfections were performed with Lipofectamine 2000 (Invitrogen) essentially as described previously (53). For imaging cells were plated on poly-L-lysine- and collagen-coated glass-bottom culture dishes in DMEM with 1% (v/v) serum, and neuronally differentiated with 100 ng/ml 7S mouse nerve growth factor for 4 days as described previously (32). Primary cortical cultures were prepared from cerebral cortices of mouse embryos (day 14-16 of gestation) and cultured as described previously (52). The cultures were obtained by breeding C57BL/6 mice. Cells were plated at 5×10^3 cells/cm² on polylysine- and laminin-coated coverslips. Sindbis virus was applied at 9 days *in vitro* and the cell fixation was performed 24 h later as described previously (52).

Immunocytochemistry

Immunocytochemistry after fixation with 4% paraformaldehyde was performed as described previously (17) using the anti-tau antibody from chicken. Fluorescence microscopy was performed using an oil-immersion 40× (NA 1.0) objective lens on a fluorescence microscope (Eclipse TE2000-U; Nikon) equipped with a digital camera (COOL-1300; Vosskühler). Infected cells were classified by visual inspection for the presence of tau or MAP2 in neuronal processes. The axonal process was identified by morphological criteria as described previously (32).

Expression of tau and annexin in yeast

The constructs that were expressed in yeast are described in Table 1. In short, recombinant tau constructs were expressed in the yeast strain DHD5 (54) from episomal vectors based on YEp352 (2 μ m, *URA3* (55)) under the control of the *GAL1/10* promoter (pJH447 (56)). The coding sequences for full-length AnxA2-GFP fusion protein, the AnxA2

core domain (35-339), the AnxA2 N-terminal region (1-34) or AnxA6 were expressed under the control of the constitutive *PFK2* promoter (57) from a vector based on YEplac181 (2 μ m, *LEU2* (58)). Smaller fragments of tau were produced as fusion proteins with the yeast phosphoglycerate mutase Gpm1 (59).

GFP pull-down assays

For preparation of yeast extracts, cells were grown overnight in 5 ml synthetic complete medium with 2% glucose (w/v) with omissions of uracil and/or leucine as required for selection of plasmid maintenance. These cultures were used to inoculate 50 ml of fresh synthetic complete medium with 2% galactose (w/v) as a sole carbon source for high-level expression of the tau constructs, and incubated for another 14-15 h at 30°C with shaking. Cells were harvested by centrifugation and washed twice with buffer (50 mM potassium phosphate buffer, pH 7.0), prior to the preparation of crude extracts with glass beads, as described previously (50). Yeast extracts were prepared from yeast cells expressing recombinant GFP or GFP-annexin constructs, and untagged or 2HA-tagged tau constructs in lysis buffer (10 mM Tris-HCl, 150 mM NaCl, 0.15% NP-40, pH 7.5) in the presence or absence of 1 mM CaCl₂. Lysates were diluted to 500 μ l with immunoprecipitation (IP) buffer (10 mM Tris-HCl, 150 mM NaCl, and 1 mM PMSF, pH 7.5) with or without 1 mM CaCl₂. Pull-down assays were performed with GFP-Trap_A beads (ChromoTek) as described previously (17). In short, 50 μ l of the lysates (“input”) were saved, the remaining lysate was incubated with the GFP-Trap_A beads, and GFP or GFP-fusion proteins were pulled-down by centrifugation. 50 μ l of the supernatant (“supernat.”) were saved. The pellet was washed, resuspended in 100 μ l 2 \times SDS-sample buffer, and the immunocomplexes were dissociated from the beads by boiling. Beads were separated by centrifugation and the supernatant was saved (“GFP pull down”). For immunoblot analysis, 2% of the lysate (“input”) and 10% each of the “supernat.” and “GFP pull down” fraction were loaded, and detected as described previously (60).

Bioinformatic analysis

pHMM was generated by HMMBUILD from collected and manually curated MAPT amino acid sequences and visualized as a HMM logo by the SKYLIGN package (61,62). The HMM of mammals (49 sequences) was compared with the HMM of other classes (Aves, 15 sequences; Reptilia, 12 sequences; Actinopterygii, 15 sequences). A potential three-dimensional (3D) structure of tau (441-aa isoform) was generated by Random Coil Generator (RCG) software (63) and the domain organization was mapped onto the 3D structure. Visualization and structure rendering was performed using the Visual Molecular Dynamics package as surface representation (64). The random coil model is frequently used to generate conformational ensembles of IDPs.

Live imaging and FDAP analysis of tau-microtubule interaction

Live imaging was performed using a laser scanning microscope (Eclipse TE2000-U inverted; Nikon, Tokyo, Japan) equipped with argon (488-nm) and violet diode (407-nm) lasers. PAGFP-tau-expressing cells were visualized with a Fluor 60 \times (NA 1.4) ultraviolet-corrected objective lens. The microscope was enclosed in an incubation chamber maintained at 37°C and 5% CO₂ (Solent Scientific, Fareham, United Kingdom). Photoactivation of a neurite’s segment of 6 μ m in length and automated image acquisition of 112 frames after photoactivation with a frame rate of 1/s was performed as described previously (33). Analysis of individual FDAP curves to estimate directly the pseudo-first-order association rate (k_{on}^*) and the dissociation rate (k_{off}) of tau to/from microtubules was performed as described previously (32).

Other methods

Preparation of PC12 cell lysates, protein determination, SDS-PAGE and immunoblot analysis by enhanced chemiluminescence were performed as described previously (32). Statistical analysis was performed using Student’s t-test for comparing two means or one-way ANOVA with Tukey’s posthoc for multiple comparison. The α -levels were defined as follows: * p <0.05, ** p <0.01, *** p <0.001.

ACKNOWLEDGEMENTS

We thank Drs. Roman Efremov and Anton Chugunov (M.M. Shemyakin & Yu.A. Ovchinnikov Institute of Bioorganic Chemistry, Russian Academy of Sciences, Moscow, Russia) for estimations concerning a potential model for the tau-annexin interaction, and Vanessa Herkenhoff for technical assistance. The work was supported by the DAAD (“Deutscher Akademischer Austauschdienst”) and performed as part of the IPID (“International Promovieren in Deutschland”) doctoral student exchange program from the University of Osnabrück and the University of Oviedo, the FICYT (“Fundación para el Fomento en Asturias de la Investigación Científica Aplicada y la Tecnología”), by computing time by the HLRN (“Norddeutscher Verbund für Hoch- und Höchstleistungsrechnen”), the UV2000/GPU cluster at the computing center of the University of Osnabrück, and the Z-project of the SFB 944, University of Osnabrück.

CONFLICT OF INTEREST

The authors declare that they have no conflicts of interest with the contents of this article.

AUTHOR CONTRIBUTIONS

AGK, MSA, FS, BN, LB and RB contributed to the acquisition, analysis, and interpretation of data; JJH, MPF and RB contributed to the conception and design of the work; RB was drafting the work. All authors revised the work critically and approved the final version of the manuscript.

REFERENCES

1. Chapin, S. J., and Bulinski, J. C. (1992) Microtubule stabilization by assembly-promoting microtubule-associated proteins: a repeat performance. *Cell Motil Cytoskeleton* **23**, 236-243
2. Binder, L. I., Frankfurter, A., and Rebhun, L. I. (1985) The distribution of tau in the mammalian central nervous system. *J Cell Biol* **101**, 1371-1378
3. Kempf, M., Clement, A., Faissner, A., Lee, G., and Brandt, R. (1996) Tau binds to the distal axon early in development of polarity in a microtubule- and microfilament-dependent manner. *J Neurosci* **16**, 5583-5592
4. Mandell, J. W., and Banker, G. A. (1996) A spatial gradient of tau protein phosphorylation in nascent axons. *J Neurosci* **16**, 5727-5740
5. Dixit, R., Ross, J. L., Goldman, Y. E., and Holzbauer, E. L. (2008) Differential regulation of dynein and kinesin motor proteins by tau. *Science* **319**, 1086-1089
6. Spillantini, M. G., and Goedert, M. (2013) Tau pathology and neurodegeneration. *Lancet Neurol* **12**, 609-622
7. Li, X., Kumar, Y., Zempel, H., Mandelkow, E. M., Biernat, J., and Mandelkow, E. (2011) Novel diffusion barrier for axonal retention of Tau in neurons and its failure in neurodegeneration. *EMBO J* **30**, 4825-4837
8. Sun, X., Wu, Y., Gu, M., Liu, Z., Ma, Y., Li, J., and Zhang, Y. (2014) Selective filtering defect at the axon initial segment in Alzheimer's disease mouse models. *Proc Natl Acad Sci U S A* **111**, 14271-14276
9. Sohn, P. D., Tracy, T. E., Son, H. I., Zhou, Y., Leite, R. E., Miller, B. L., Seeley, W. W., Grinberg, L. T., and Gan, L. (2016) Acetylated tau destabilizes the cytoskeleton in the axon initial segment and is mislocalized to the somatodendritic compartment. *Mol Neurodegener* **11**, 47
10. Marin, M. A., Ziburkus, J., Jankowsky, J., and Rasband, M. N. (2016) Amyloid-beta plaques disrupt axon initial segments. *Exp Neurol* **281**, 93-98
11. Uversky, V. N. (2015) Intrinsically disordered proteins and their (disordered) proteomes in neurodegenerative disorders. *Front Aging Neurosci* **7**, 18
12. Gunawardana, C. G., Mehrabian, M., Wang, X., Mueller, I., Lubambo, I. B., Jonkman, J. E., Wang, H., and Schmitt-Ulms, G. (2015) The Human Tau Interactome: Binding to the

- Ribonucleoproteome, and Impaired Binding of the Proline-to-Leucine Mutant at Position 301 (P301L) to Chaperones and the Proteasome. *Mol Cell Proteomics* **14**, 3000-3014
13. Konzack, S., Thies, E., Marx, A., Mandelkow, E. M., and Mandelkow, E. (2007) Swimming against the tide: mobility of the microtubule-associated protein tau in neurons. *J Neurosci* **27**, 9916-9927
 14. Janning, D., Igaev, M., Sundermann, F., Bruhmann, J., Beutel, O., Heinisch, J. J., Bakota, L., Piehler, J., Junge, W., and Brandt, R. (2014) Single-molecule tracking of tau reveals fast kiss-and-hop interaction with microtubules in living neurons. *Mol Biol Cell* **25**, 3541-3551
 15. Brandt, R., Leger, J., and Lee, G. (1995) Interaction of tau with the neural plasma membrane mediated by tau's amino-terminal projection domain. *J Cell Biol* **131**, 1327-1340
 16. Weissmann, C., Reyher, H. J., Gauthier, A., Steinhoff, H. J., Junge, W., and Brandt, R. (2009) Microtubule binding and trapping at the tip of neurites regulate tau motion in living neurons. *Traffic* **10**, 1655-1668
 17. Gauthier-Kemper, A., Weissmann, C., Golovyashkina, N., Sebo-Lemke, Z., Drewes, G., Gerke, V., Heinisch, J. J., and Brandt, R. (2011) The frontotemporal dementia mutation R406W blocks tau's interaction with the membrane in an annexin A2-dependent manner. *J Cell Biol* **192**, 647-661
 18. Gerke, V., Creutz, C. E., and Moss, S. E. (2005) Annexins: linking Ca²⁺ signalling to membrane dynamics. *Nat Rev Mol Cell Biol* **6**, 449-461
 19. Rescher, U., and Gerke, V. (2004) Annexins--unique membrane binding proteins with diverse functions. *J Cell Sci* **117**, 2631-2639
 20. Bharadwaj, A., Bydoun, M., Holloway, R., and Waisman, D. (2013) Annexin A2 heterotetramer: structure and function. *Int J Mol Sci* **14**, 6259-6305
 21. Zhao, W. Q., and Lu, B. (2007) Expression of annexin A2 in GABAergic interneurons in the normal rat brain. *J Neurochem* **100**, 1211-1223
 22. Yamatani, H., Kawasaki, T., Mita, S., Inagaki, N., and Hirata, T. (2010) Proteomics analysis of the temporal changes in axonal proteins during maturation. *Dev Neurobiol* **70**, 523-537
 23. Sanchez-Ponce, D., DeFelipe, J., Garrido, J. J., and Munoz, A. (2011) In vitro maturation of the cisternal organelle in the hippocampal neuron's axon initial segment. *Mol Cell Neurosci* **48**, 104-116
 24. Eberhard, D. A., Brown, M. D., and VandenBerg, S. R. (1994) Alterations of annexin expression in pathological neuronal and glial reactions. Immunohistochemical localization of annexins I, II (p36 and p11 subunits), IV, and VI in the human hippocampus. *Am J Pathol* **145**, 640-649
 25. Hamre, K. M., Chepenik, K. P., and Goldowitz, D. (1995) The annexins: specific markers of midline structures and sensory neurons in the developing murine central nervous system. *J Comp Neurol* **352**, 421-435
 26. Porzig, R., Singer, D., and Hoffmann, R. (2007) Epitope mapping of mAbs AT8 and Tau5 directed against hyperphosphorylated regions of the human tau protein. *Biochem Biophys Res Commun* **358**, 644-649
 27. Sundermann, F., Fernandez, M. P., and Morgan, R. O. (2016) An evolutionary roadmap to the microtubule-associated protein MAP Tau. *BMC Genomics* **17**, 264
 28. Hayashi, S., Toyoshima, Y., Hasegawa, M., Umeda, Y., Wakabayashi, K., Tokiguchi, S., Iwatsubo, T., and Takahashi, H. (2002) Late-onset frontotemporal dementia with a novel exon 1 (Arg5His) tau gene mutation. *Ann Neurol* **51**, 525-530
 29. Poorkaj, P., Muma, N. A., Zhukareva, V., Cochran, E. J., Shannon, K. M., Hurtig, H., Koller, W. C., Bird, T. D., Trojanowski, J. Q., Lee, V. M., and Schellenberg, G. D. (2002) An R5L tau mutation in a subject with a progressive supranuclear palsy phenotype. *Ann Neurol* **52**, 511-516
 30. Lee, G., Thangavel, R., Sharma, V. M., Litersky, J. M., Bhaskar, K., Fang, S. M., Do, L. H., Andreadis, A., Van Hoesen, G., and Ksiezak-Reding, H. (2004) Phosphorylation of tau by fyn: implications for Alzheimer's disease. *J Neurosci* **24**, 2304-2312
 31. Gerke, V., and Moss, S. E. (2002) Annexins: from structure to function. *Physiol Rev* **82**, 331-371

32. Niewidok, B., Igaev, M., Sundermann, F., Janning, D., Bakota, L., and Brandt, R. (2016) Presence of a carboxy-terminal pseudorepeat and disease-like pseudohyperphosphorylation critically influence tau's interaction with microtubules in axon-like processes. *Mol Biol Cell* **27**, 3537-3549
33. Igaev, M., Janning, D., Sundermann, F., Niewidok, B., Brandt, R., and Junge, W. (2014) A refined reaction-diffusion model of tau-microtubule dynamics and its application in FDAP analysis. *Biophys J* **107**, 2567-2578
34. Dotti, C. G., Sullivan, C. A., and Banker, G. A. (1988) The establishment of polarity by hippocampal neurons in culture. *J Neurosci* **8**, 1454-1468
35. Maas, T., Eidenmuller, J., and Brandt, R. (2000) Interaction of tau with the neural membrane cortex is regulated by phosphorylation at sites that are modified in paired helical filaments. *J Biol Chem* **275**, 15733-15740
36. Liu, C., Song, X., Nisbet, R., and Gotz, J. (2016) Co-immunoprecipitation with Tau Isoform-specific Antibodies Reveals Distinct Protein Interactions and Highlights a Putative Role for 2N Tau in Disease. *J Biol Chem* **291**, 8173-8188
37. Hirokawa, N., Shiomura, Y., and Okabe, S. (1988) Tau proteins: the molecular structure and mode of binding on microtubules. *J Cell Biol* **107**, 1449-1459
38. Heinisch, J. J., and Brandt, R. (2016) Signaling pathways and posttranslational modifications of tau in Alzheimer's disease: the humanization of yeast cells. *Microb Cell* **3**, 135-146
39. Stern, J. L., Lessard, D. V., Hoepflich, G. J., Morfini, G. A., and Berger, C. L. (2017) Phosphoregulation of Tau modulates inhibition of kinesin-1 motility. *Mol Biol Cell* **28**, 1079-1087
40. Hall, G. F., Yao, J., and Lee, G. (1997) Human tau becomes phosphorylated and forms filamentous deposits when overexpressed in lamprey central neurons in situ. *Proc Natl Acad Sci U S A* **94**, 4733-4738
41. Paquet, D., Bhat, R., Sydow, A., Mandelkow, E. M., Berg, S., Hellberg, S., Falting, J., Distel, M., Koster, R. W., Schmid, B., and Haass, C. (2009) A zebrafish model of tauopathy allows in vivo imaging of neuronal cell death and drug evaluation. *J Clin Invest* **119**, 1382-1395
42. Orr, M. E., Garbarino, V. R., Salinas, A., and Buffenstein, R. (2015) Sustained high levels of neuroprotective, high molecular weight, phosphorylated tau in the longest-lived rodent. *Neurobiol Aging* **36**, 1496-1504
43. Xia, D., Gutmann, J. M., and Gotz, J. (2016) Mobility and subcellular localization of endogenous, gene-edited Tau differs from that of over-expressed human wild-type and P301L mutant Tau. *Sci Rep* **6**, 29074
44. Hatch, R. J., Wei, Y., Xia, D., and Gotz, J. (2017) Hyperphosphorylated tau causes reduced hippocampal CA1 excitability by relocating the axon initial segment. *Acta Neuropathol* **133**, 717-730
45. Kneynsberg, A., and Kanaan, N. M. (2017) Aging Does Not Affect Axon Initial Segment Structure and Somatic Localization of Tau Protein in Hippocampal Neurons of Fischer 344 Rats. *eNeuro* **4**
46. Mercken, M., Grynspan, F., and Nixon, R. A. (1995) Differential sensitivity to proteolysis by brain calpain of adult human tau, fetal human tau and PHF-tau. *FEBS Lett* **368**, 10-14
47. Park, S. Y., and Ferreira, A. (2005) The generation of a 17 kDa neurotoxic fragment: an alternative mechanism by which tau mediates beta-amyloid-induced neurodegeneration. *J Neurosci* **25**, 5365-5375
48. Lang, A. E., Riederer, D. N., and Ferreira, A. (2014) Neuronal degeneration, synaptic defects, and behavioral abnormalities in tau(4)(5)(-)(2)(3)(0) transgenic mice. *Neuroscience* **275**, 322-339
49. Pchitskaya, E., Popugaeva, E., and Bezprozvanny, I. (2017) Calcium signaling and molecular mechanisms underlying neurodegenerative diseases. *Cell Calcium*

50. Rodicio, R., Koch, S., Schmitz, H. P., and Heinisch, J. J. (2006) KIRHO1 and KIPKC1 are essential for cell integrity signalling in *Kluyveromyces lactis*. *Microbiology* **152**, 2635-2649
51. Maeder, C. I., Hink, M. A., Kinkhabwala, A., Mayr, R., Bastiaens, P. I., and Knop, M. (2007) Spatial regulation of Fus3 MAP kinase activity through a reaction-diffusion mechanism in yeast pheromone signalling. *Nat Cell Biol* **9**, 1319-1326
52. Bakota, L., Brandt, R., and Heinisch, J. J. (2012) Triple mammalian/yeast/bacterial shuttle vectors for single and combined Lentivirus- and Sindbis virus-mediated infections of neurons. *Mol Genet Genomics* **287**, 313-324
53. Fath, T., Eidenmuller, J., and Brandt, R. (2002) Tau-mediated cytotoxicity in a pseudohyperphosphorylation model of Alzheimer's disease. *J Neurosci* **22**, 9733-9741
54. Kirchrath, L., Lorberg, A., Schmitz, H. P., Gengenbacher, U., and Heinisch, J. J. (2000) Comparative genetic and physiological studies of the MAP kinase Mpk1p from *Kluyveromyces lactis* and *Saccharomyces cerevisiae*. *J Mol Biol* **300**, 743-758
55. Hill, J. E., Myers, A. M., Koerner, T. J., and Tzagoloff, A. (1986) Yeast/*E. coli* shuttle vectors with multiple unique restriction sites. *Yeast* **2**, 163-167
56. Lorberg, A., Schmitz, H. P., Jacoby, J. J., and Heinisch, J. J. (2001) Lrg1p functions as a putative GTPase-activating protein in the Pkc1p-mediated cell integrity pathway in *Saccharomyces cerevisiae*. *Mol Genet Genomics* **266**, 514-526
57. Raben, N., Exelbert, R., Spiegel, R., Sherman, J. B., Nakajima, H., Plotz, P., and Heinisch, J. (1995) Functional expression of human mutant phosphofructokinase in yeast: genetic defects in French Canadian and Swiss patients with phosphofructokinase deficiency. *Am J Hum Genet* **56**, 131-141
58. Gietz, R. D., and Sugino, A. (1988) New yeast-*Escherichia coli* shuttle vectors constructed with in vitro mutagenized yeast genes lacking six-base pair restriction sites. *Gene* **74**, 527-534
59. Heinisch, J., von Borstel, R. C., and Rodicio, R. (1991) Sequence and localization of the gene encoding yeast phosphoglycerate mutase. *Curr Genet* **20**, 167-171
60. Leschik, J., Welzel, A., Weissmann, C., Eckert, A., and Brandt, R. (2007) Inverse and distinct modulation of tau-dependent neurodegeneration by presenilin 1 and amyloid-beta in cultured cortical neurons: evidence that tau phosphorylation is the limiting factor in amyloid-beta-induced cell death. *J Neurochem* **101**, 1303-1315
61. Eddy, S. R. (1998) Profile hidden Markov models. *Bioinformatics* **14**, 755-763
62. Wheeler, T. J., Clements, J., and Finn, R. D. (2014) Skylign: a tool for creating informative, interactive logos representing sequence alignments and profile hidden Markov models. *BMC Bioinformatics* **15**, 7
63. Jha, A. K., Colubri, A., Freed, K. F., and Sosnick, T. R. (2005) Statistical coil model of the unfolded state: resolving the reconciliation problem. *Proc Natl Acad Sci U S A* **102**, 13099-13104
64. Humphrey, W., Dalke, A., and Schulten, K. (1996) VMD: visual molecular dynamics. *J Mol Graph* **14**, 33-38, 27-38

TABLE 1: List of constructs expressed in yeast.

| Expression plasmid | Insert | Backbone / Promoter | Comment |
|--------------------|------------------------------|-------------------------|---|
| pJJH1207 | GFP | YEplac181 / <i>PFK2</i> | control without annexin |
| pJJH1190 | AnxA2-GFP | YEplac181 / <i>PFK2</i> | |
| pJJH1443 | AnxA2(1-34)-GFP | YEplac181 / <i>PFK2</i> | |
| pJJH1431 | AnxA2(35-339)-GFP | YEplac181 / <i>PFK2</i> | |
| pJJH1597 | AnxA6-GFP | YEplac181 / <i>PFK2</i> | |
| pJJH900 | Flag τ 441wt | YEp352 / <i>GALI-10</i> | |
| pJJH1283 | 2HA-Flag τ 441wt | YEp352 / <i>GALI-10</i> | |
| pJJH1288 | 2HA-Flag τ (1-255) | YEp352 / <i>GALI-10</i> | |
| pJJH1441 | 2HA- τ (256-441) | YEp352 / <i>GALI-10</i> | no Flag-tag |
| pJJH1289 | 2HA-Flag τ (1-171) | YEp352 / <i>GALI-10</i> | |
| pJJH1418 | 2HA-Flag τ (1-44)-Gpm1 | YEp352 / <i>GALI-10</i> | the short tau peptide itself is unstable in yeast, thus the fusion with a small glycolytic enzyme |
| pJJH2236 | 2HA- τ (1-44)-Gpm1 | YEp352 / <i>GALI-10</i> | Same as pJJH1418 but without Flag-tag |
| pJJH1439 | 2HA-Gpm1 | YEp352 / <i>GALI-10</i> | control without tau |
| pJJH1494 | 2HA-Flag τ (1-171;R5H) | YEp352 / <i>GALI-10</i> | |
| pJJH1496 | 2HA-Flag τ (1-171;R5L) | YEp352 / <i>GALI-10</i> | |
| pJJH1541 | 2HA-Flag τ (1-171;Y18F) | YEp352 / <i>GALI-10</i> | |
| pJJH1542 | 2HA-Flag τ (1-171;Y18E) | YEp352 / <i>GALI-10</i> | |

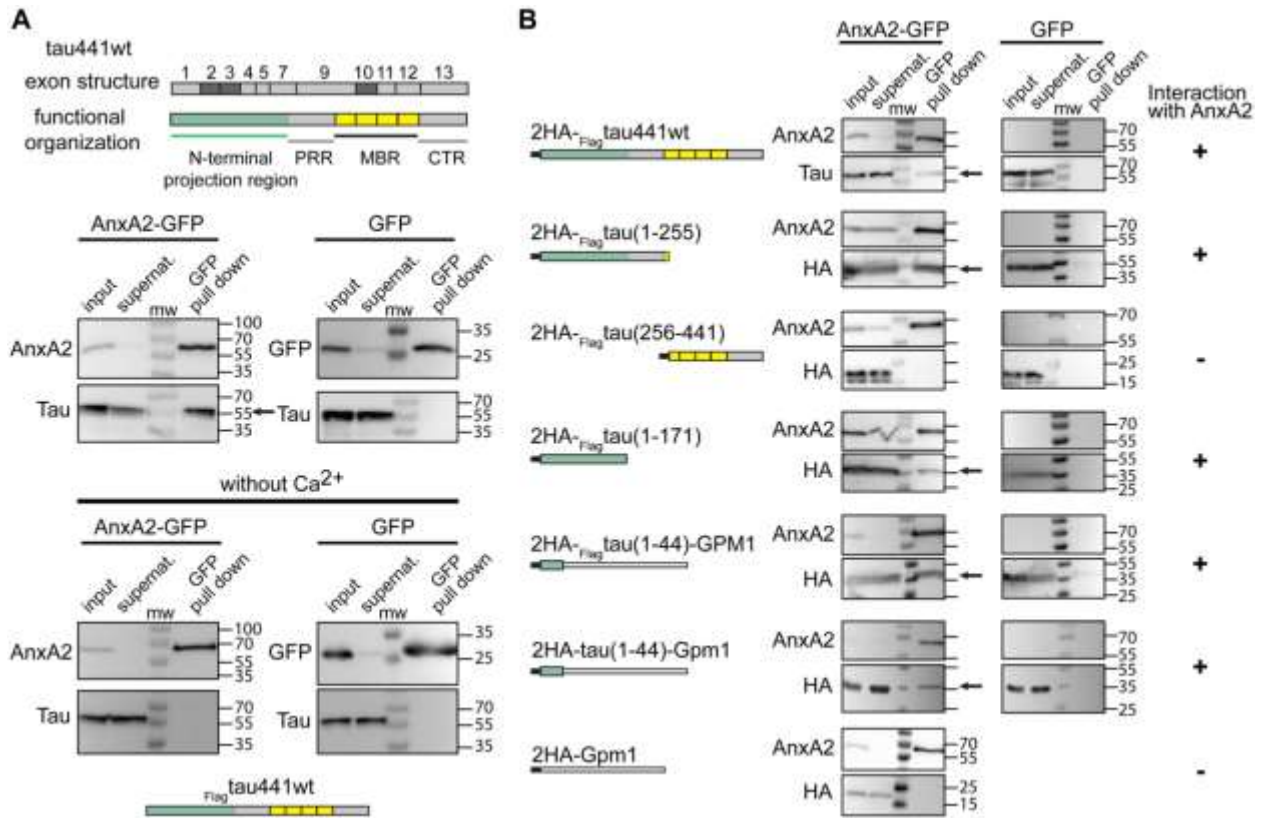


Figure 1: Tau interacts with AnxA2 through E1.

A. Exon structure of tau441wt with conventional nomenclature is shown on top. Exons that are alternatively spliced in the CNS are indicated in dark gray. Tau's functional organization is shown below. The repeat regions, which constitute the basic microtubule interacting unit, are indicated in yellow, the N-terminal projection domain in light green. Immunoblots showing the result of pull-down assays of exogenously expressed tau and annexin A2 (AnxA2) in the presence or absence of calcium ions in the heterologous yeast system are displayed below. Tau co-precipitated after pull-down of AnxA2-GFP in the presence, but not absence of Ca²⁺ (bottom left). No co-precipitation was observed in control experiments (pull-down of GFP; middle right). Numbers at the sides of the gel blots indicate molecular mass standards in kilodaltons. CTR, C-terminal region; MBR, microtubule-binding region, PRR, proline-rich region. **B.** Pull-down assays of annexin (AnxA2-GFP) and controls (GFP) with 2HA-tagged tau and a panel of tau deletion constructs. Tau-deletion constructs containing the sequence of E1 (amino acids 1-44) co-precipitated after pull down of AnxA2-GFP, while the C-terminal half (256-441) or the carrier (Gpm1) did not. All co-precipitation experiments were confirmed by at least two independent experiments.

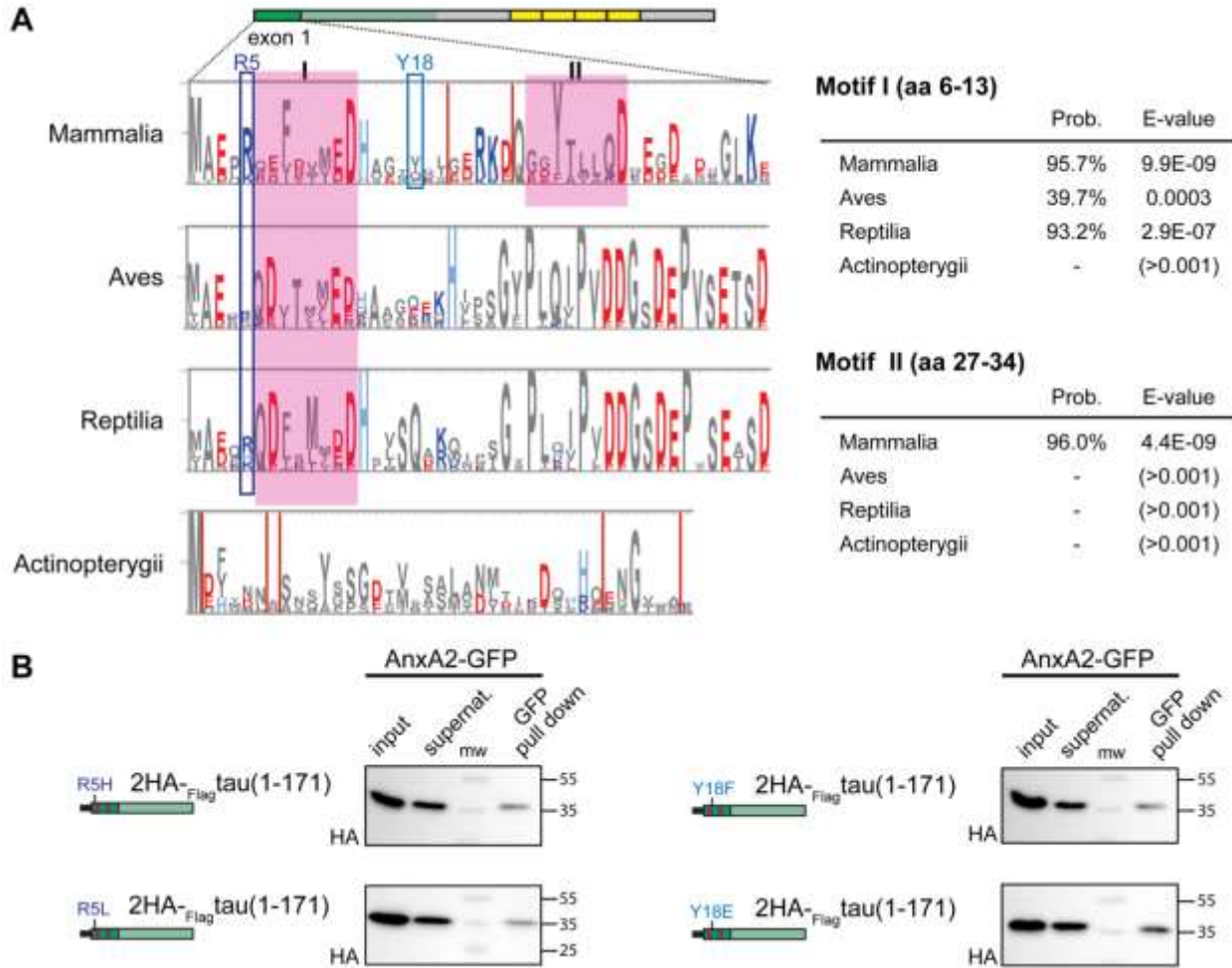


Figure 2: Bioinformatic analysis and effects of familial and phospho-site mutations on tau's binding to AnxA2.

A. pHMM logo of E1 of mammalian tau and pHMMs of birds (Aves), reptiles (Reptilia) and ray-finned fishes (Actinopterygii). Conserved motifs are indicated by boxes in magenta and designated as I and II. Acidic amino acids are represented in red, basic ones in blue color. Positions where individual amino acids are mutated in tauopathies and where potentially disease-relevant tyrosine-phosphorylation had been reported are indicated by blue boxes. Probabilities (Prob.) and expectation values (E-values) for the two motifs are indicated right. **B.** Pull-down assays of annexin (GFP-AnxA2) with the HA-tagged tau projection region (1-171) harboring FTDP-17 mutations R5H and R5L (left) and phospho blocking and mimicking mutations of tyrosine 18 (Y18F, Y18E) (right). The mutated constructs co-precipitated to a similar extent (quantitation of bound versus total signal revealed $13.6\pm 9.4\%$ and $15.7\pm 13.8\%$ for Y18F and Y18E, respectively, and $15.0\pm 5.1\%$ and $15.7\pm 9.4\%$ for R5H and R5L constructs, respectively; mean \pm SD (n=3)). E1 is indicated in dark green with the conserved sequence motifs shown in magenta.

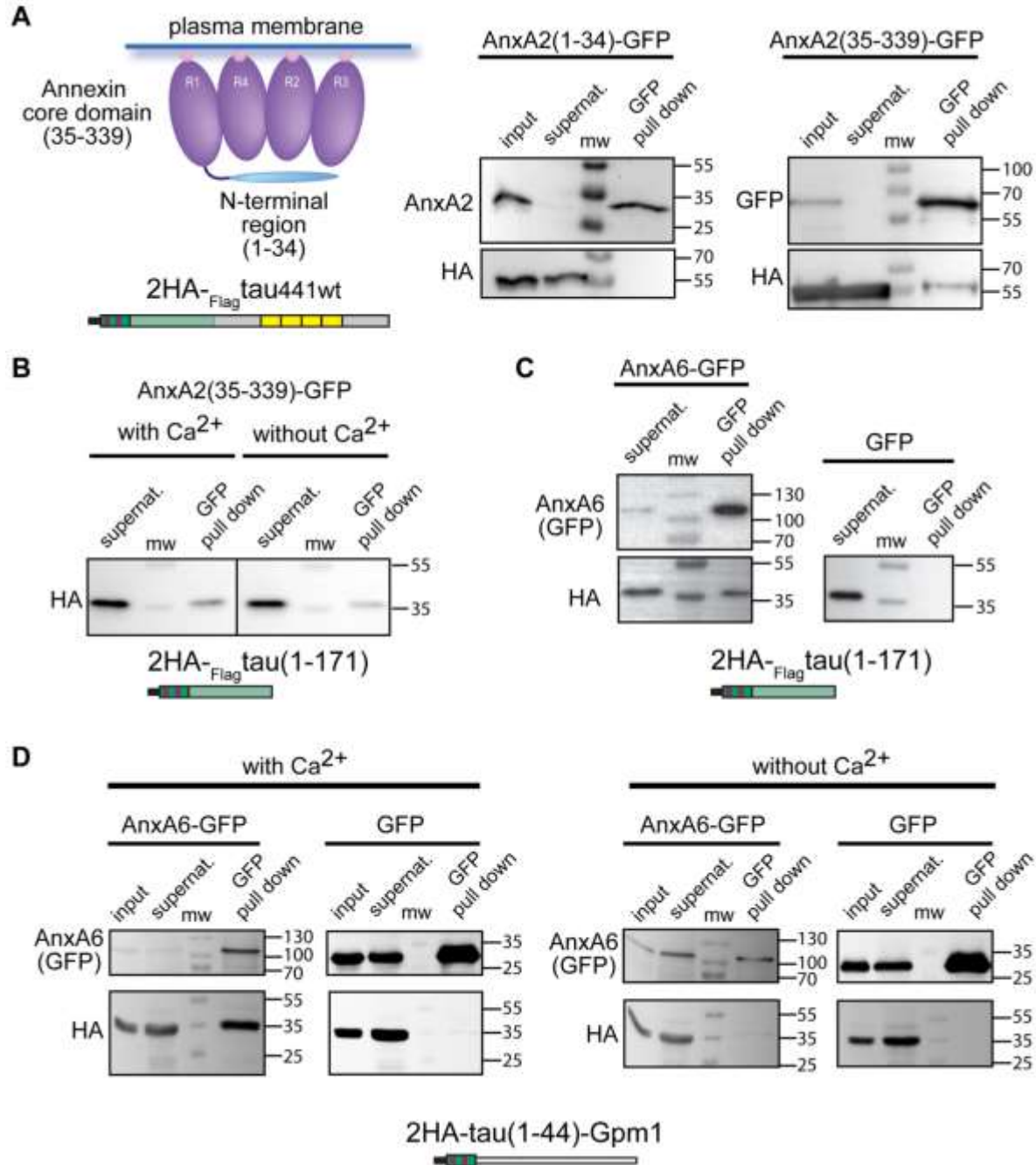


Figure 3: Tau binds to the core domain of AnxA2 and also interacts with AnxA6.

A. Pull-down assays of the core domain of AnxA2 (AnxA2(35-339)-GFP) and the N-terminal region (AnxA2(1-34)-GFP) with HA-tagged tau. A schematic representation of the structure of annexinA2 is shown top left. Annexin repeats (R1-R4) of the core domain are indicated. Ca-ions are indicated as pink balls. **B.** Pull-down assays of the core domain of AnxA2 (AnxA2(35-339)-GFP) with the HA-tagged tau project region (1-171) in the presence or absence of Ca²⁺. Tau interacts with the core domain of AnxA2 independent of the presence of Ca²⁺. The schematic structure of tau is color-coded as described in the legend of Figure 2. **C, D.** Pull-down assays of AnxA6 (AnxA6-GFP) with the HA-tagged tau projection region (1-171) (C) or HA-tagged tau(1-44)-Gpm1 (D) indicate co-precipitation of tau. Binding of AnxA6 to E1 requires the presence of Ca²⁺ (D).

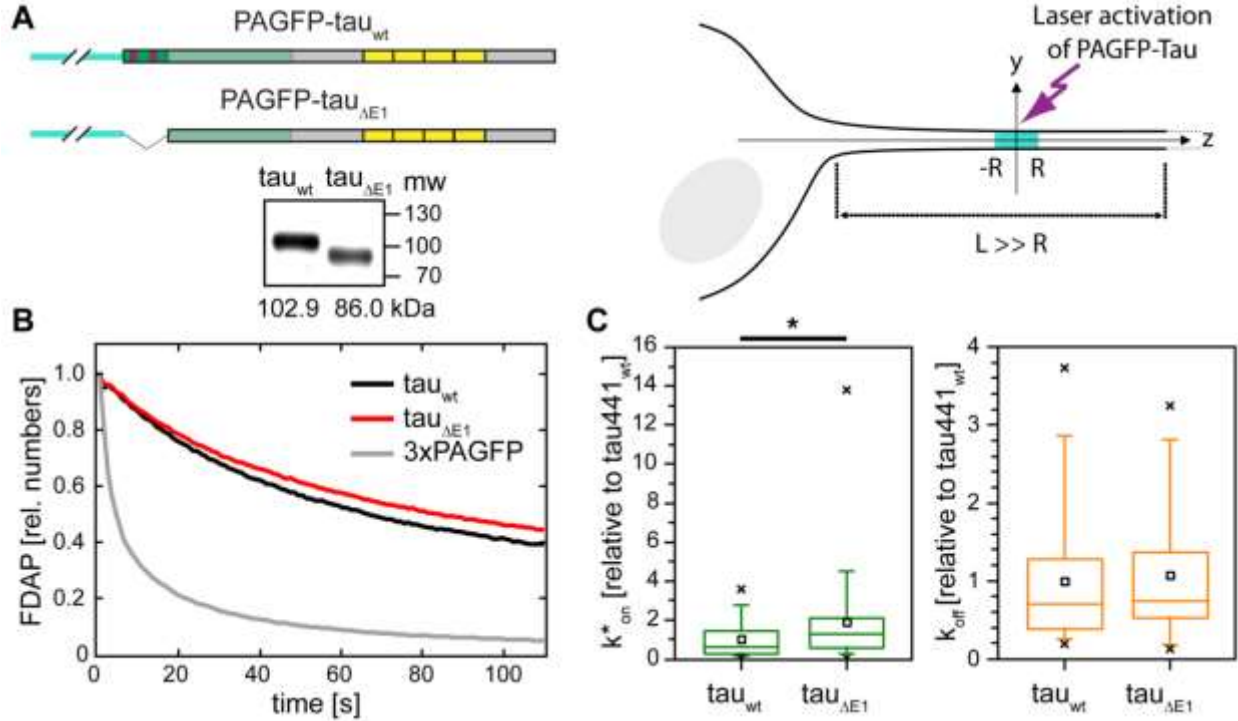


Figure 4: Lack of E1 moderately increases tau's association rate with microtubules in axon-like processes.

A. Schematic representation of wildtype tau (τ_{wt}) and a tau deletion construct lacking first coding exon ($\tau_{\Delta E1}$) with N-terminal PAGFP-fusion. The PAGFP-tag is indicated in turquoise, the schematic structure of tau is color-coded as described in the legend of Figure 2. An immunoblot of cellular lysates after transfection with the respective tau constructs is shown below. Molecular weights as determined from the electrophoretic separation are indicated below. A schematic representation of the photoactivation approach is shown to the right. Photoactivation was performed in neuronally differentiated PC12 cells. A segment $2R$ in length in the middle of a cellular process of length L ($L \gg R$) was photoactivated, and the fluorescence distribution was monitored over time. **B.** FDAP plots of PAGFP-tagged τ_{wt} , $\tau_{\Delta E1}$ and $3 \times \text{PAGFP}$ as a non-MT binding control of similar size are shown. Curves represent the mean values of 30-43 experiments. **C.** Bar plots showing k_{on}^* and k_{off} values of τ_{wt} and $\tau_{\Delta E1}$. The numbers are expressed relative to τ_{wt} . The box represents 50% of the population, whiskers range from 5 to 95%, crosses correspond to the minimal and maximal values, the horizontal line shows the median and the black squares show the mean value. Statistical analysis was performed using Student's t-test. Statistically significant differences between the means are indicated. *, $p < 0.05$ ($n=39$ and 43 for τ_{wt} and $\tau_{\Delta E1}$, respectively).

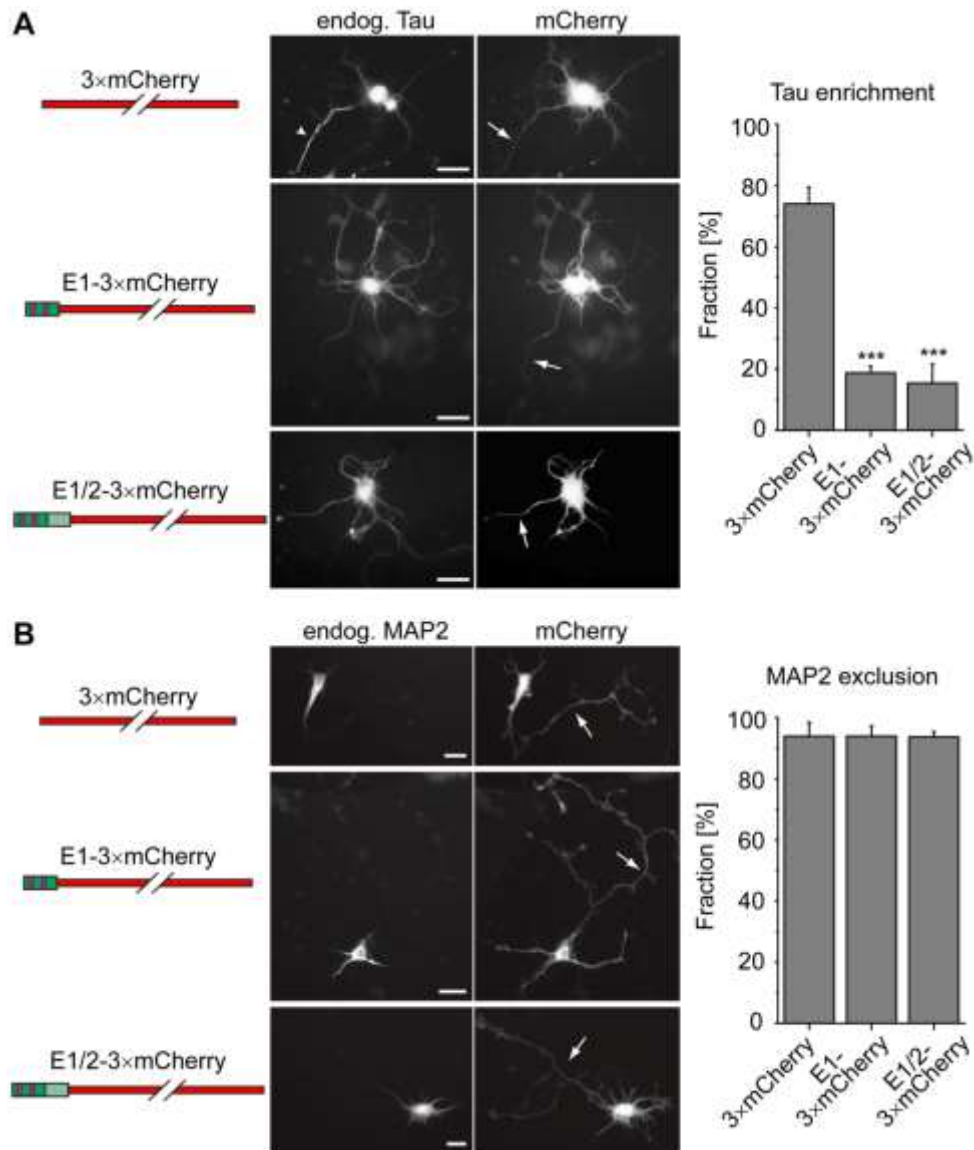


Figure 5: Overexpression of tau's E1 decreases axonal retention of endogenous tau but does not affect MAP2 exclusion from the axon.

A. Distribution of endogenous tau in primary cortical mouse neurons after viral overexpression of the indicated constructs. Representative fluorescence micrographs are shown in the middle. Arrows indicate axons in the infected neurons as they are evident by morphological criteria. The arrowhead indicates axonal enrichment of tau after expression of the control construct (3×mCherry), which is not present after expression of sequence including tau's first exon (E1). Quantification of the fraction of infected neurons, which exhibit axonal tau enrichment, is shown on the right. **B.** Distribution of endogenous MAP2 in neurons overexpressing the indicated constructs. Arrows indicate axons. Note the exclusion of MAP2 from the axon after expression of all constructs. Quantification of the fraction of infected neurons, which exhibit axonal exclusion of MAP2, is shown on the right. Tau and MAP2 distribution were classified by visual inspection of a total of 129-199 (tau) and 117-146 (MAP2) infected neurons per construct from four independent experiments. Values are shown as mean \pm SD. Statistical analysis was performed using one-way ANOVA with Tukey's posthoc for multiple comparison. ***, $p < 0.001$, compared to the control experiment (expression of 3×mCherry) for tau enrichment; statistical analysis revealed no significant difference between the constructs for MAP2 distribution. Scale bar, 20 μ m.

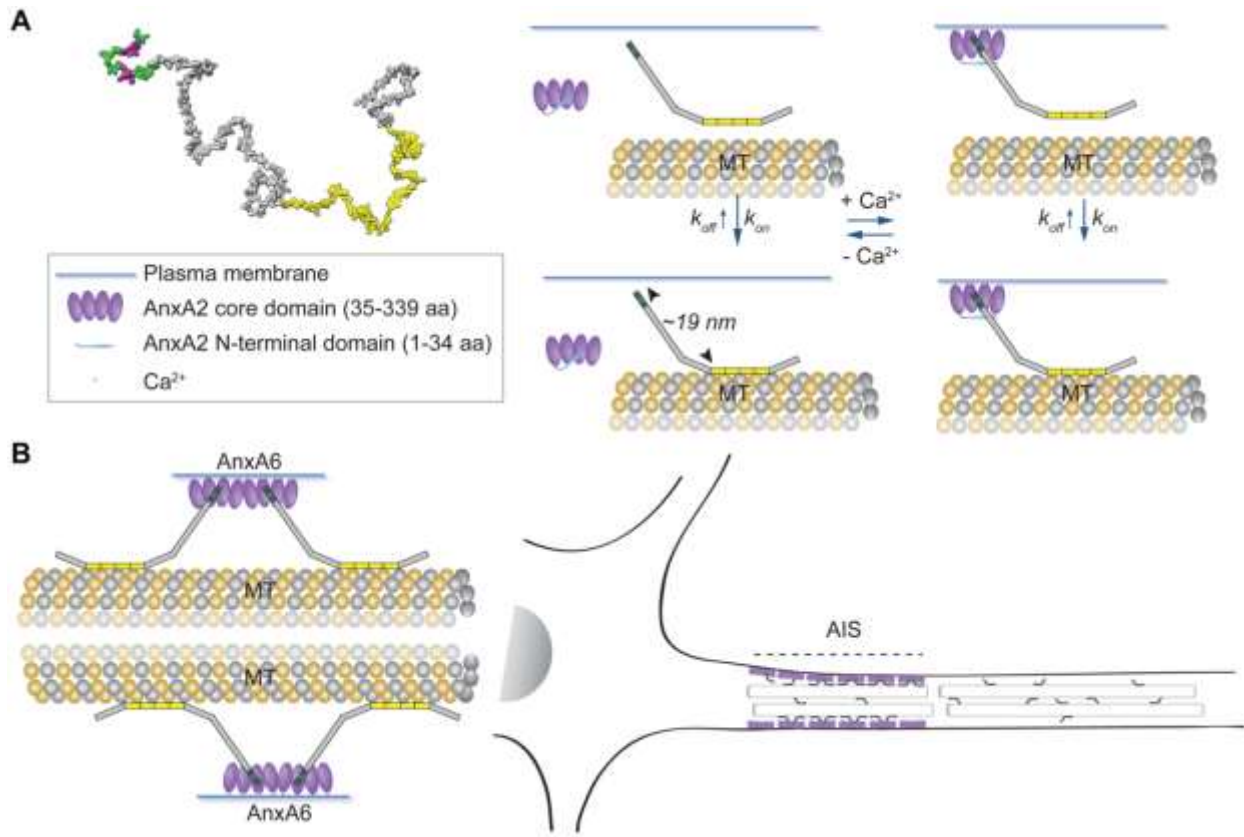


Figure 6: Schematic representation visualizing the major findings of the study.

A. Potential 3D structure of tau (tau441wt) based on the RCG model. The MBD (yellow) and the position of exon 1 (dark green) together with the two evolutionary conserved sequence motifs (magenta) were mapped on the structure. The end-to-end distance (distance between amino acids 1 and 441) is ~25 nm. Tau interacts with the core-domain of AnxA2 via the first exon of its amino-terminal projection domain in a Ca²⁺-dependent manner. The interaction with annexin moderately reduces k_{on} . Tau links microtubules to the axonal plasma membrane through its aminoterminal projection domain, which protrudes ~19 nm from the MT surface. **B.** Tau interacts also with AnxA6, which carries two annexin cores within a single physical entity. AnxA6 localizes to the axon initial segment (AIS), where binding of tau may produce a bottle-neck contributing to the retention of tau in the axonal compartment of higher vertebrates.